

# Reports

## What Perturbs the $\gamma$ and $\delta$ Rings of Uranus?

R. G. FRENCH, J. A. KANGAS, J. L. ELLIOT

The  $\gamma$  and  $\delta$  rings have by far the largest radial perturbations of any of the nine known Uranian rings. These two rings deviate from Keplerian orbits, having typical root-mean-square residuals of about 3 kilometers (compared to a few hundred meters for the other seven known rings). Possible causes for the perturbations include nearby shepherd satellites and Lindblad resonances. If shepherd satellites are responsible, they could be as large as several tens of kilometers in diameter. The perturbation patterns of the  $\gamma$  and  $\delta$  rings have been examined for evidence of Lindblad resonances of azimuthal wave number  $m = 0, 1, 2, 3,$  and  $4$ . The  $\delta$  ring radial residuals are well matched by a 2:1 Lindblad resonance. If this represents a real physical phenomenon and is not an artifact of undersampling, then the most plausible interpretation is that there is an undiscovered satellite orbiting  $76,522 \pm 8$  kilometers from Uranus, with an orbital period of  $15.3595 \pm 0.0001$  hours and a radius of 75 to 100 kilometers. Such a satellite would be easily detected by the Voyager spacecraft when it encounters Uranus. The 2:1 resonance location is  $41 \pm 9$  kilometers inside the  $\delta$  ring, which makes it unlikely that the resonance is due to a viscous instability within the ring. In contrast, no low-order Lindblad resonance matches the  $\gamma$  ring perturbations, which are probably caused by one or more shepherd satellites large enough to be clearly visible in Voyager images.

SINCE THE DISCOVERY OF THE URANIAN rings in 1977 (1), a continuing series of stellar occultation observations has made it possible to determine the orbits of the rings with remarkable precision. It is now known that seven of the nine known rings follow well-behaved Keplerian ellipses, slightly inclined to the equatorial plane and precessing under the gravitational influence of the oblate planet. Typical post-fit residuals for these rings are only a few hundred meters in radius. However, two adjacent rings,  $\gamma$  and  $\delta$ , deviate significantly from simple ellipses, with residuals of up to 10 km (2). With the combination of a large data set, accurate event times, and a new kinematic model for the ring orbits, we can examine the pattern of residuals with the goal of determining the mechanism responsible for the perturbations. In this report, we restrict our attention to the  $\gamma$  and  $\delta$  rings and test two possible causes of the observed perturbations: shepherd satellites that are presumed to confine the sharp-edged narrow rings, and low-order Lindblad resonances.

According to the model of ring confinement by shepherd satellites, a passing shepherd induces a wave in the adjacent ring of wavelength

$$\lambda = 3\pi\Delta \quad (1)$$

where  $\Delta$  is the radial separation between the satellite and the ring (3). Since the  $\gamma$  and  $\delta$  rings are separated by about 670 km, a

shepherd midway between the two rings would give a wavelength of 3200 km. The circumference of each ring is about  $3 \times 10^5$  km, so that the shepherd wake would have an azimuthal wave number of roughly 100. For shepherd satellites with smaller  $\Delta$ , the wave number would be even higher. This makes a direct search for a shepherd wake infeasible with the present data set, which is too sparse to permit unique identification of a shepherd satellite in the perturbation pattern because of severe undersampling. Furthermore, a shepherd wake may be damped over a distance that is small compared to the ring circumference, so that its signature would be occasional large, but for the most part well-behaved, residuals. We need only look at the images of Saturn's F ring to realize that narrow rings can have large and complex radial perturbations (4).

The best we can do at present is relate the observed root-mean-square (rms) perturbation amplitude to the size and location of a putative shepherd satellite. The result for the  $\gamma$  and  $\delta$  rings is that shepherds of radius

$$r \approx \frac{60 \text{ km}}{\rho^{1/3}} \left[ \frac{\Delta}{10 \text{ km}} \right]^{2/3} \quad (2)$$

could perturb the rings to the observed extent (5). Here,  $\rho$  is the density of the satellite in grams per cubic centimeter. Since the perturbations are as large as 10 km for the  $\gamma$  ring, it is unlikely that  $\Delta$  is smaller than 10 km. If shepherd satellites are solely responsible for the perturbations seen in the  $\gamma$

and  $\delta$  rings, then they are likely to have radii of 10 km or greater.

Unlike shepherd satellites, low-order Lindblad resonances produce regular variations in ring radius that are sufficiently large scale to allow a direct search to be made in the available data. Global observations of the 22 April 1982 occultation suggest that radius residuals of the  $\gamma$  and  $\delta$  rings vary more slowly with ring longitude than expected from shepherd satellites (6). The condition for a Lindblad resonance is that

$$m(\Omega - \Omega_f) = \Omega - \dot{\bar{\omega}} \quad (3)$$

where  $\Omega$  is the mean motion at resonance,  $\Omega_f$  is the pattern speed,  $\dot{\bar{\omega}}$  is the mean precession rate at resonance due to the planetary gravitational field, and  $m$  is the azimuthal wave number (Eq. 3 is valid for  $m \neq 0$ ; the  $m = 0$  mode corresponds to a radial oscillation of epicyclic frequency  $\dot{\bar{\omega}}$ ). We have in mind a Lindblad resonance with a small satellite inside the orbit of Miranda, in which case  $\Omega_f$  represents the angular velocity of the satellite. There are a number of such resonances in the Saturn ring system, such as the Mimas 2:1 Lindblad resonance at 1.95 Saturn radii ( $R_S$ ) and the 7:6 coorbital Lindblad resonance at 2.27  $R_S$  (7). As another possibility, instabilities within a ring itself may show such resonant characteristics if the ring particles are near close-packed (8). In this case,  $\Omega$  would be the mean motion of a particle within the ring.

In a coordinate frame rotating at a speed  $\Omega_f$ , the radial perturbation amplitude for a Lindblad resonance with  $m \neq 0$  is given by

$$\Delta r = \frac{C_m}{|a - a_r|} \cos m(\phi - \phi_0) \quad (4)$$

where  $a$  is the semimajor axis of the ring and  $a_r$  is the radius of the Lindblad resonance.  $C_m$  is proportional to the ratio of the satellite and planetary masses ( $M_S/M_U$ ) and to a factor of order unity that depends on the specific resonance in question (9);  $\phi$  is ring longitude measured with respect to an inertial reference line and  $\phi_0$  is the phase offset at a specified epoch. For the  $m = 0$  mode, the perturbation amplitude is given by

$$\Delta r \propto \cos[(\Omega - \dot{\bar{\omega}})(t - t_{\text{ref}}) - \phi_0] \quad (5)$$

where  $t$  is the time of the observation and  $t_{\text{ref}}$  is a reference time at which the phase of the disturbance is  $\phi_0$ . If the  $m = 0$  mode is the result of an internal instability within the ring, then the proportionality constant im-

R. G. French, Department of Earth, Atmospheric, and Planetary Sciences, Massachusetts Institute of Technology, Cambridge 02139.

J. A. Kangas, Department of Physics, Massachusetts Institute of Technology, Cambridge 02139.

J. L. Elliot, Department of Earth, Atmospheric, and Planetary Sciences and Department of Physics, Massachusetts Institute of Technology, Cambridge 02139.

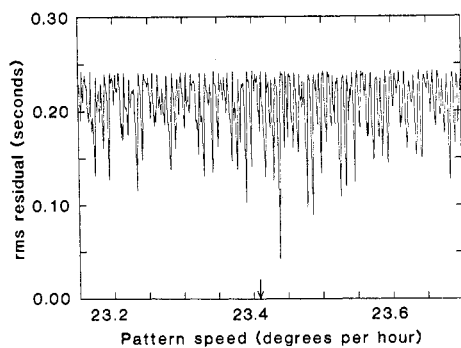


Fig. 1. Scan for Lindblad resonances in the vicinity of the  $\delta$  ring for azimuthal wave number  $m = 2$ . The arrow marks the pattern speed  $\Omega_f$  appropriate for an internal instability within the ring. The deep minimum in the post-fit residuals at  $\Omega_f = 23.4383$  degrees per hour may be indicative of a small satellite inside the orbit of Miranda.

plicit in Eq. 5 is related to dissipative processes within the ring. If, on the other hand, the  $m = 0$  mode is excited by an external satellite in a noncircular orbit, then  $\Delta r$  is proportional to the mass and orbital eccentricity of the satellite.

Using all the available observations of the  $\gamma$  and  $\delta$  rings (10), we searched for Lindblad resonances that could account in detail for the large observed radial perturbations, modeling the ring on the basis of Eqs. 4 and 5. Our procedure was, for each wave number  $m$ , to determine the range of pattern speeds  $\Omega_f$  corresponding to a resonance radius  $a_r$  that is within a few hundred kilometers of the semimajor axis of the ring, and for each pattern speed, to determine the corresponding amplitude  $C_m$ , phase  $\phi_0$ , and mean ring radius that give the best match to the observations. (For  $m = 0$ , we scanned through a range of epicyclic frequencies rather than through  $\Omega_f$ .) The rms residual from the fit was then plotted as a function of pattern speed, and a search was made for a solution that is consistent with the detailed residual pattern of each ring. This is analogous to the method used to scan for precession rates of the elliptical Uranian rings (11).

Such a search reveals whether the large residuals of the  $\gamma$  and  $\delta$  rings can be accounted for by any large-scale sinusoidal perturbation rotating at a constant pattern speed over the 8 years of available observations. In effect, this represents a normal-mode analysis of the perturbation patterns and is not tied to any specific physical mechanism. Nevertheless, if the perturbations were caused by an undiscovered satellite, the solution would determine its location to high accuracy and provide an estimate of its mass.

Using the procedure described above, we searched for Lindblad resonances of azimuthal wave number  $m = 0, 1, 2, 3$ , and 4 over appropriate ranges of frequencies for

both the  $\gamma$  and  $\delta$  rings. Because typical pattern speeds are tens of degrees per hour, and because observations are infrequent, one might anticipate substantial aliasing in the results of the scans. (An exception is the  $m = 1$  mode, which corresponds to a Keplerian ellipse precessing at a few degrees per day as a result of the harmonics of the planetary gravitational field.) On the other hand, multiple observations of a given occultation provide important constraints on models for longitudinal ring structure. This is because there is nearly simultaneous sampling of ring radius at the widely separated immersion and emersion ring longitudes, as well as mapping variations over scales of roughly 5000 km by virtue of the north-south separation of the observatories.

For the  $\gamma$  ring, we found no Lindblad resonances that can match the observed perturbations with an rms residual less than 0.2 second. Even when the unperturbed ring was allowed to be inclined and eccentric (adding 4 d.f. to the fit), the best fit had an rms residual of more than 0.09 second, which is significantly greater than typical post-fit residuals for the "well-behaved" rings 6, 5, 4,  $\alpha$ ,  $\beta$ ,  $\eta$ , and  $\epsilon$ . The  $\delta$  ring scans for  $m = 0, 1, 3$ , and 4 do not show good fits to the observed perturbations. In contrast, there is a deep minimum for the  $m = 2$  scan (Fig. 1) for  $\Omega_f = 23.4383$  degrees per hour.

We suggest that the minimum reflects a true 2:1 Lindblad resonance, and is not simply a spurious fit to sparse data, for the following reasons.

1) The pattern speed of the best fit is near the location of the  $\delta$  ring 2:1 resonance. If the fit were spurious, there would be no reason to expect the best fit to occur at a physically significant pattern speed.

2) In spite of the evident aliasing, the best fit has an rms residual less than half as large as the next best fit. Furthermore, the rms residual for the best fit is 0.04 second, which is comparable to the post-fit residuals to the best fit to the  $\epsilon$  ring, for example (12).

3) If the excellent fit is due purely to undersampling, we would expect to see equally good fits for other azimuthal wave numbers  $m$  at arbitrary pattern speeds. These are not seen. It is not easy to estimate the a priori probability of obtaining a spurious but formally excellent fit to the observations, because the distribution of data points is not random over the 8-year interval during which the observations were made: data points are separated by hours (for immersion and emersion events during a single stellar occultation) as well as months and years. As a test of the uniqueness of the best fit, we scanned pattern speeds from 0 to 30 degrees per hour for the  $\delta$  ring  $m = 2$  mode. There were no comparably good fits over

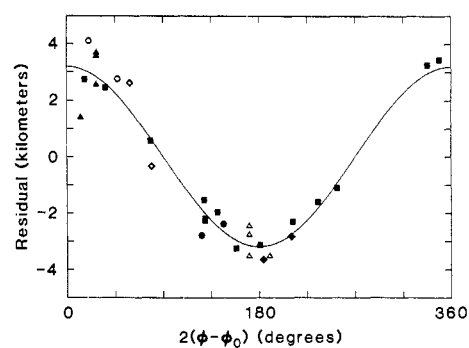


Fig. 2. Radius residuals of the  $\delta$  ring ( $m = 2$ ). The symbols indicate the observed radius residuals, and the solid line is the best fitting  $m = 2$  Lindblad perturbation with a pattern speed of  $\Omega_f = 23.4383$  degrees per hour, plotted as a function of longitude in the frame of reference rotating at  $\Omega_f$ . Typical error bars in radius are a few tenths of a kilometer. Multiple observations of the same occultation are shown as follows: ( $\Delta$ ,  $\blacktriangle$ ) 22 April 1982; ( $\circ$ ,  $\bullet$ ) 4 May 85; ( $\diamond$ ,  $\blacklozenge$ ) 24 May 1985. In each case the unfilled symbols represent immersion and the filled symbols represent emersion. All other observations are shown as ( $\blacksquare$ ).

this entire range; the second-best fit had an rms residual greater than 0.07 second.

4) When the unperturbed ring was allowed to be eccentric and inclined (adding an additional 4 d.f. to the fit), the results were not substantially different from those shown in Fig. 1.

If this is regarded as a true resonance phenomenon, it is probably not caused by internal instabilities within the ring of the sort suggested by Borderies and co-workers because the resonance location is near, but not at, the  $\delta$  ring radius (13). However, a small satellite inside the orbit of Miranda could be responsible for the perturbations. Under this interpretation, we calculated the orbital elements and size of such a satellite (Table 1). There is an ambiguity of  $\pm 180^\circ$  in satellite longitude, owing to the centered elliptical perturbation pattern of an  $m = 2$  Lindblad resonance. Figure 2 shows the observed residuals to the best-fitting unperturbed circular equatorial ring, plotted as a function of the azimuthal angle  $m(\phi - \phi_0)$  (Eq. 4) for the Lindblad resonance in Table 1. From the radial perturbation amplitude  $\Delta r$  obtained from the best fit, we found that the predicted satellite radius for the best fit to the data is 75 to 100 km for a range of densities of 1 to 3 g cm $^{-3}$  (14).

In addition to statistical arguments about the significance of the observed minimum in the  $\delta$  ring 2:1 Lindblad resonance search, several independent tests of the satellite hypothesis have occurred to us.

1) Could such a satellite have escaped prior detection? The most thorough searches for small inner Uranian satellites have

Table 1. Results of best fit to  $\delta$  ring residuals.

Parameter	Value
<i>Proposed satellite</i>	
Semimajor axis	76,522 $\pm$ 8 km
Orbital period	15.3595 $\pm$ 0.0001 hours
Mean motion $\Omega_f$	23.4383 $\pm$ 0.0001 degrees per hour
Longitude $\phi_0$	221 $\pm$ 4 degrees*
Mass	(4 $\pm$ 1) $\times$ 10 <sup>21</sup> g
<i>Lindblad resonance</i>	
Azimuthal wave number ( $m$ )	2
Resonance radius ( $a_r$ )	48,265 $\pm$ 8 km
( $a_r - a$ )	-41 $\pm$ 9 km
$C_m$	120 $\pm$ 6 km <sup>2</sup>
$\Delta r$	3.2 $\pm$ 0.2 km

\*There is a  $\pm 180^\circ$  uncertainty in the longitude, which is measured in a prograde sense from the western section of the line of intersection of Earth's and Uranus' equatorial planes at 20:00 (universal time) on 10 March 1977.

made use of charge-coupled device (CCD) images. At a distance of 2.92  $R_U$ , corresponding to the orbital radius of the proposed satellite, observations in the I band give an upper limit of a few hundred kilometers in radius for a satellite having a geometrical albedo  $p_I$  of 0.2 (15). CCD observations at 2.2  $\mu\text{m}$  (K band) with a detection limit of about 125 km in satellite radius for a geometrical albedo  $p_K$  of 0.25 have been made for a small region of the sky near Uranus (16); no satellites were found. [These geometrical albedos are typical of the four large satellites of Uranus (17).] We conclude that the proposed satellite is too small to have been detected with the best Earth-based observations.

2) Would the satellite cause unacceptably large perturbations in the adjacent rings? The radial perturbation amplitude  $\Delta r$  is inversely proportional to the separation between the ring radius and the resonance location,  $|a - a_r|$ . Since  $|a - a_r|$  is 41 km for the suspected resonance, and the distance to the  $\gamma$  ring (the closest neighbor) is about 670 km, the perturbation at the  $\gamma$  ring would be 0.2 km, which is much smaller than the observed characteristic perturbation of about 3 km. Therefore, the proposed satellite would not produce detectable perturbations in the other rings.

3) Could the proposed resonance account for the observed variations in ring width? If the shape of a streamline in a coordinate system rotating at  $\Omega_f$  is given by

$$r = a[1 - \epsilon(a) \cos m(\phi - \phi_0)] \quad (6)$$

then, to first order, the ring width can be expressed as

$$\delta r = \delta a - a \delta \epsilon \cos m(\phi - \phi_0) \quad (7)$$

where  $\delta a$  is the mean ring width and  $\delta \epsilon$  is the difference in eccentricity between the inner and outer edges of the ring. Since ring widths have been determined from fits to most of the occultation profiles used in the resonance searches, it is possible in principle

to compare the observed width variations of the  $\delta$  ring with these predicted by a given Lindblad resonance by fitting for  $\delta a$  and  $\delta \epsilon$ .

We performed a series of such fits for the range of pattern speeds given in Fig. 1 for the  $\delta$  ring 2:1 Lindblad resonance, but we found no good fits to the data. This is not surprising, since the variation in ring width expected from a Lindblad resonance can be shown to be of order  $\delta a \Delta r / |a - a_r|$ , which is less than 0.4 km in this case, compared to observed width variations of several kilometers for the  $\delta$  ring. In other words, the observed variations in the width of the  $\delta$  ring are much larger than could naturally be explained by a Lindblad resonance. Furthermore, all the nine Uranian rings have been shown to have significant width perturbations (2). In particular, rings 6, 5, and 4, which are of comparable width to the  $\delta$  ring, do not satisfy Eq. 7 for  $m = 1$ , even though their elliptical orbits have been established to high precision. Whatever mechanism is producing the large width variations in these three rings may also be at work in the  $\delta$  ring.

4) Are multiple observations of the same occultation consistent with the proposed resonance? Three occultations have been observed from widely separated sites: 22 April 1982 and 4 and 24 May 1985. Figure 2 shows the distribution of residuals for these observations as a function of perturbation longitude. In most cases, the points follow the predicted perturbation pattern within the accuracy of the data. The 22 April 1982 emersion observations are an important exception. The Lindblad resonance alone cannot account for the observed pattern in these radius residuals. This may be evidence that there are significant short-wavelength radial perturbations in the  $\delta$  ring in addition to the longer wavelength resonant perturbations, perhaps caused by a shepherd satellite that is responsible for the large  $\gamma$  ring radial residuals. The alternative

is that the inferred Lindblad resonance is spurious, which seems unlikely in view of the statistical arguments given above but which cannot be ruled out as a possibility.

The  $\gamma$  and  $\delta$  rings have by far the largest radial perturbations of any of the Uranian rings and are thus best suited for resonance searches. The available observations can neither rule out nor confirm that the perturbations are due solely to shepherd satellites, but if shepherds are responsible, they may well be the largest shepherds in the Uranian ring system. We have been able to search for low wave number Lindblad resonances due to internal instabilities or small satellites inside the orbit of Miranda. The 2:1 resonance near the  $\delta$  ring is the best candidate for a Lindblad resonance, and if it is real, it is probably associated with a satellite 75 to 100 km in radius and orbiting 76,522 km from Uranus.

Our search for Lindblad resonances appears to rule out internal viscous instabilities as the primary cause of the perturbations, because the pattern speeds appropriate for such instabilities do not result in good fits to the observations. We conclude that small satellites are responsible. If our proposed satellite at 76,522 km is real, then it should be easily detected by the Voyager camera during the encounter with Uranus. Direct imaging would allow an estimate to be made of the satellite's radius and albedo, which combined with our estimated mass would provide useful clues about its composition. If the apparent 2:1 Lindblad resonance near the  $\delta$  ring is spurious, then we expect shepherd satellites tens of kilometers in diameter to be found by Voyager in the vicinity of both the  $\gamma$  and  $\delta$  rings. If their orbits could be well determined, the Earth-based occultation observations should be reexamined to relate the perturbation amplitude and longitudinal pattern to the satellite location. This may make it possible to quantify the dissipative processes involved in damping the shepherd wake.

#### REFERENCES AND NOTES

1. J. L. Elliot, E. W. Dunham, D. J. Mink, *Nature (London)* **267**, 328 (1977).
2. R. G. French, J. L. Elliot, S. E. Levine, in preparation.
3. J. N. Cuzzi *et al.*, in *Planetary Rings*, R. Greenberg and A. Brahic, Eds. (Univ. of Arizona Press, Tucson, 1984), pp. 73-199.
4. B. A. Smith *et al.*, *Science* **212**, 163 (1981).
5. A. Freedman, S. D. Tremaine, J. L. Elliot, *Astron. J.* **88**, 1053 (1983).
6. See figures 3 and 4 in (2).
7. C. Porco, G. E. Danielson, P. Goldreich, J. B. Holberg, A. L. Lane, *Icarus* **60**, 17 (1984).
8. N. Borderies, P. Goldreich, S. Tremaine, *ibid.* **63**, 406 (1985).
9. P. Goldreich and S. Tremaine, *ibid.* **34**, 240 (1978).
10. In addition to the observations described in (2), we have included preliminary data from the 4 and 24 May 1985 stellar occultations by Uranus, described briefly by R. G. French *et al.* [*Bull. Am. Astron. Soc.* **17**, 718 (1985)].
11. J. L. Elliot *et al.*, *Astron. J.* **86**, 444 (1981).

12. See Table 12 in (2).  
 13. A systematic error of 41 km in the radii of all nine Uranian rings would be required in order for the resonance radius to match the  $\delta$  ring radius. The estimated uncertainty in the  $\delta$  ring semimajor axis is about 5 km (2).  
 14. The estimate of the satellite mass is based on a streamline formalism that does not take into account damping due to particle collisions. Consequently, the predicted satellite size is approximate.  
 15. B. A. Smith, in *Proceedings of the Uranus and Neptune Workshop, NASA Conf. Publ. 2330*, (1984), p. 213.  
 16. P. D. Nicholson, *ibid.*, p. 589.  
 17. R. H. Brown *et al.*, *Nature (London)* 300, 423 (1982).  
*Nature (London)* 300, 423 (1982).

18. We thank S. Tremaine for helpful discussions and for suggesting that we search for Lindblad resonances and S. Levine for helping with the data analysis. Supported in part by grants NAGW-656 and NSG-7526 from The National Aeronautics and Space Administration.

20 November 1985; accepted 26 December 1985

## Model for the Intrusion of Batholiths Associated with the Eruption of Large-Volume Ash-Flow Tuffs

JAMES A. WHITNEY AND JOHN C. STORMER, JR.

Pyroclastic eruption and the intrusion of batholiths associated with large-volume ash-flow tuffs may be driven by a decrease in reservoir pressure caused by the low density of the magma column due to vesiculation. Batholithic intrusion would then be accomplished by the subsidence and settling of kilometer-sized crustal blocks through the magma chamber, resulting in eventual collapse to form large caldera structures at the surface. Such a model does not require the formation of a large, laterally extensive, shallow magma chamber before the onset of large-volume ash-flow eruptions. Eruption could commence directly from a deeper reservoir, with only a small channelway being opened to the surface before the onset of catastrophic ash-flow eruptions of the scale of Yellowstone or Long Valley. Such a model has wide-ranging implications, and explains many of the problems inherent in the simple collapse model involving shallow magma chambers as well as the process and timing of batholith intrusion in such cases.

**I**N THIS REPORT WE OUTLINE A MODEL for the emplacement of batholiths and the eruption mechanism for large-volume ash-flow tuffs. Because this model satisfies many of the physical data now available, and since it has dramatic implications for volcanic hazards and hydrothermal power projects, it should be considered as a possible alternative to the shallow magma chamber collapse model currently being proposed for all caldera-forming events.

The emplacement of batholiths has always been a problem in geology because of the need to explain where the original rocks went. Since the magma comes from below, some process must cause crustal subsidence to offset the upward movement of the magma. Large-volume ash flows such as the Bishop (1), Yellowstone (2), and San Juan Mountains (3) tuffs represent 500 to 3000 km<sup>3</sup> of material, implying magma systems of batholithic proportions (a batholith is a minimum of 100 km<sup>2</sup> in outcrop area; most are not more than 5 km thick). Since many batholiths are accompanied by cogenetic ash-flow tuffs immediately before their final emplacement, both share common origins and should be intimately related in intrusive and extrusive history.

A second problem is that a number of

recent ash-flow eruptions do not seem to have left behind extensive and continuous shallow magma chambers, as would be suggested by the current model of caldera collapse into a preexisting shallow chamber (4). Therefore the question must be asked, where did the magma go?

As silicic magma coalesces in the lower crust, it will begin to rise diapirically when the body becomes large enough (5). This type of upward migration depends on the surrounding material being plastic because of high temperatures and confining pressures. As the magma moves upward, it must soften the surrounding rocks by heating before continued movement is possible (5). There is increasing geophysical evidence to suggest that this process leads to a ponding of magmas in the mid-crust, where the rocks become cooler and more brittle (4, 6). Geochemical evidence also suggests that the magma chemistry of batholiths represents crystal reequilibration at mid-crustal depths (7). The present model therefore starts with a large concentration of magma at depths of 10 to 20 km.

The density contrasts that lead to diapiric upwelling still exist, and cause distension of the overlying crust and propagation of outward fractures (Fig. 1A). The process is driven by the pressure differential between the upper part of the magma body and the surrounding rocks. The lower crustal rocks below the body are plastic, having been

preheated. They push in on the lower margin with a pressure corresponding to the local geobaric conditions. Since the magma is a fluid, although a rather viscous one, pressure is transmitted to the upper surface where the magma pressure is equal to the lithostatic pressure at the base minus the magma column pressure. This pressure is higher than the local lithostatic pressure at the top by the term

$$P = 98.0655 \int_0^L \Delta\rho dl \quad (1)$$

where  $L$  is the thickness of the body in kilometers and  $\Delta\rho$  is the difference between the magma density and that of the country rock as a function of depth. If we assume that the densities do not vary much over the thickness of the body, then Eq. 1 simplifies to

$$P = 98.0655\Delta\rho L \quad (2)$$

The resulting pressure differential is about 100 bars per 1 g/cm<sup>3</sup> of density differential for every 1 km in thickness. This force will aid crack propagation in the tensional environment, especially if preexisting zones of weakness are utilized, as is generally the case in the localization of plutons.

Crack propagation therefore progresses into the brittle environment, with fingers of magma expanding ring fractures toward the surface (Fig. 1A). Such a process is now occurring under the Mammoth Lakes area in California (4, 8).

Eventually, the magma will reach the surface. If the magma channelway is big enough, large volumes of magma may begin to be extruded as pyroclastic material, provided there are sufficient volatiles to drive the eruption. At this point, the fluid pressure in the magma chamber changes. If a significant amount of material is moving up the column, the pressure in the magma chamber will attempt to reach the pressure of the flowing magma column, which is given by the expression

$$P = 98.0655 \int_0^H \rho_m dh \quad (3)$$

where  $\rho_m$  is the density of the magma in grams per cubic centimeter and  $H$  is the

J. A. Whitney, Department of Geology, University of Georgia, Athens 30602.  
 J. C. Stormer, Jr., Department of Geology and Geophysics, Rice University, P.O. Box 1892, Houston, TX 77251.